Implicit numerical integration of an advanced subloading surface clay and sand model

Paul J. Pinedo[1,2], Mohamed Rouainia[2], Lluís Monforte[3], Marcos Arroyo[1,3], Antonio Gens[1,3]

[1]*Dept. of Civil and Environmental Engineering, Universitat Politècnica de Catalunya - BarcelonaTech (UPC)*
Carrer de Jordi Girona, 31, 08034, Barcelona, Spain
paul.jose.pinedo@upc.edu, marcos.arroyo@upc.edu, antonio.gens@upc.edu
[2]*School of Civil Engineering and Geosciences, Newcastle University*
Drummond Building, NE1 7RU, Newcastle upon Tyne, UK
mohamed.rouainia@newcastle.ac.uk
[3]*Geomechanics Group, Centre Internacional de Mètodes Numèrics en Enginyeria (CIMNE)*
C/ Gran Capitán S/N UPC Campus Nord, Edifici C1, 08034, Barcelona, Spain
lluis.monforte@upc.edu

Abstract. This paper focuses on the algorithmic and computational aspects of implementing the clay and sand model (CASM) using a fully implicit numerical scheme. CASM is a unified critical state model that relies on the state parameter concept and incorporates a non-associated flow rule. Within this framework, the subloading enhancement is introduced, which enables a smooth elastic-plastic transition through an isotropic modification. The addition of just one extra parameter significantly enhances the calibration process. Subsequently, the modified version of CASM is implemented into a finite element procedure. The demonstrate the efficiency and good performance of the proposed algorithm, including the subloading modification, simulations of triaxial compression tests under undrained conditions are conducted.

Keywords: clay and sand model (CAMS), subloading, plasticity, implicit integration, finite element.

1 Introduction

Classical elasto-plastic constitutive models can capture the constitutive response of soils. However, several limitations have been frequently reported: the yield surface is too large, they predict a drastic shift between elastic and elasto-plastic regimes, and they fail to predict the accumulation of strains during long amplitude cyclic loading (Wichtmann et al. [1]). An existing constitutive model might be extended to introduce these realistic soil behaviour features by reformulating it in the framework of subloading surface plasticity (Hashiguchi [2, 3]; Hashiguchi et al. [4]; Hashiguchi [5]) or bounding surface plasticity (Rouainia and Muir-Wood [6]).

Robust and efficient stress integration techniques are thus required to use these constitutive models for numerical simulations of boundary value problems. There are several procedures to compute the stress increment given a strain increment, such as explicit integration (Sloan et al. [7]) or implicit methods, in which the return algorithms are probably the most well-known method (Simo and Hughes [8]). Explicit stress integration schemes have been employed to extend existing elastoplastic constitutive models to the subloading surface approach, for instance, the modified Cam-Clay model (Pedroso [9]) and CASM (Pinedo et al. [10]). However, the main advantage of the implicit integration algorithm is that unconditionally stable, and therefore results in a quite robust scheme from the computational numerical point of view (Hashash and Whittle [11]).

Clay And Sand Model (CASM) (Yu [12]; Mánica et al. [13]; Arroyo and Gens [14]) is a model based on the classical elasto-plasticity framework. In this work, an implicit integration scheme is employed to discretize the constitutive equations of CASM extended using a subloading surface plasticity approach. Moreover, this new constitutive model is programmed in FORTRAN as a user-defined soil model (UDSM) in PLAXIS computer

application (PLAXIS [15]).

The paper is organized as follows: a summary of the CASM and its extension in the subloading surface approach, then a detailed explanation of the implicit numerical integration and, finally, the achievement of this method is evaluated in simulations of the Boston Blue Clay laboratory tests (BBC) (Braathen [16]; Pestana et al. [17]).

2 Subloading surface approach

Subloading surface plasticity, as proposed by Hashiguchi [2, 3] and Hashiguchi et al. [4], presents an unconventional plasticity framework characterized by its ability to represent the smooth transition from an elastic to a plastic regime. This approach employs two distinct yield surfaces: the subloading surface and the normal yield surface. The current stress is always situated within the subloading surface. Although both yield surfaces share the same shape, they are different in size (Hashiguchi et al. [4]). In addition, this approach induces plastic strain within the normal yield surface, allowing for the representation of hysteretic behaviour during cyclic loading. Moreover, this is accomplished by introducing an additional hardening law, consisting of one hardening variable and an extra constitutive parameter. The following section provides a summary of the extension of the CASM model to incorporate subloading surface plasticity.

Classical elasto-plasticity for small strains assumes that the strain tensor, $\boldsymbol{\epsilon}$, can be additively decomposed into its elastic and plastic parts, denoted by $\boldsymbol{\epsilon}^e$ and $\boldsymbol{\epsilon}^p$, respectively (Simo [18]). Subloading plasticity similarly preserves this strain decomposition. The elastic law is expressed in terms of both the volumetric and deviatoric components:

$$\boldsymbol{\sigma} = \mathbf{s} + p'\mathbb{1} \qquad \dot{p}' = K\dot{\epsilon}_v^e = K(\dot{\epsilon}_v - \dot{\epsilon}_v^p) \qquad \dot{\mathbf{s}} = 2G\dot{\boldsymbol{\epsilon}}_d^e = 2G(\dot{\boldsymbol{\epsilon}}_d - \dot{\boldsymbol{\epsilon}}_d^p) \tag{1}$$

where $\boldsymbol{\sigma}$ is the Cauchy stress tensor, $\boldsymbol{s}$ stands for the deviatoric stress tensor, $p' = 1/3tr\boldsymbol{\sigma}$ is the mean effective stress, $\mathbb{1}$ is the second order identity tensor, K is the bulk modulus, ϵ_v^e is the volumetric elastic strain, ϵ_v is the volumetric strain, ϵ_v^p is the volumetric plastic strain, G is the shear modulus, $\boldsymbol{\epsilon}_d^e$ is the deviatoric elastic strain, $\boldsymbol{\epsilon}_d$ represents the deviatoric strain and, $\boldsymbol{\epsilon}_d^p$ is the deviatoric plastic strain. The value of the bulk and shear moduli depend on the mean effective stress:

$$K = \frac{p'}{\kappa^*} \qquad G = \frac{3(1-2\mu)}{2(1+\mu)}K \tag{2}$$

where $\kappa^* = \kappa/(1+e_o)$ represents the slope of the swelling line in a volumetric strain-logarithmic mean stress compression plane, where e_o is the initial void ratio and, μ is the Poisson's coefficient.

The extension of the CASM to the subloading surface framework requires the definition of two yield surfaces: the normal yield surface, F, and the subloading surface, f. Both of these yield surfaces, are expressed by eq. (3)a and eq. (3)b, respectively. The equation defining the normal yield surface coincides with the yield surface of CASM based on classical elastoplasticity.

$$F = \left(\frac{\sqrt{\frac{3}{2}\mathbf{s}:\mathbf{s}}}{p'M_\theta}\right)^n + \frac{1}{\ln r}\ln\frac{p'}{p_o'} \qquad f = \left(\frac{\sqrt{\frac{3}{2}\mathbf{s}:\mathbf{s}}}{p'M_\theta}\right)^n + \frac{1}{\ln r}\ln\frac{p'}{R_s p_o'} \tag{3}$$

where M_θ represents the stress ratio at the critical state, n is a parameter that determines the shape of the yield surface, r is a spacing ratio, that controls the location of the intersection of the critical state line and the yield surface, p_o' stands for the preconsolidation pressure and, R_s is the similarity ratio.

The similarity ratio, R_s, is defined as the ratio of the size of the subloading surface to that of the normal yield surface. It serves as a general measure to describe the extent of approach to the normal-yield surface (see eq. (7)) (Hashiguchi [5]). $R_s = 0$ corresponds to the null stress state, $0 < R_s < 1$ corresponds to the subyield state, and $R_s = 1$ corresponds to the normal yield state, where the stress lies on the normal yield surface (Hashiguchi et al. [4]).

For a non-associative plastic model, the flow rule may be expressed by eq. (4)a. CASM assumes a non-associative flow rule, and eq. (4)b expresses the plastic potential function, denoted as g (Mánica et al. [13]).

$$\dot{\boldsymbol{\epsilon}}^p = \dot{\gamma}\frac{\partial g}{\partial \boldsymbol{\sigma}} \qquad g = \left(\frac{\sqrt{\frac{3}{2}\mathbf{s}:\mathbf{s}}}{p' M_\theta}\right)^m + m - \frac{y(m-1)}{p'} - 1 \tag{4}$$

where $\dot{\gamma}$ denotes the plastic multiplier, m is a parameter that governs the shape of the function, and y must be solved for the current stress state.

Subloading surface plasticity differs from classical plasticity in that it assumes that the current stress state always lies on the normal yield surface and employs a more relaxed version of the Kuhn-Tucker conditions. Plastic straining occurs when the loading condition is satisfied:

$$\dot{\gamma} > 0 \quad \text{if} \quad \frac{\partial f}{\partial \boldsymbol{\sigma}} : \mathbb{D}_e : \dot{\boldsymbol{\epsilon}} > 0 \tag{5}$$

$$\dot{\gamma} = 0 \quad \text{if} \quad \frac{\partial f}{\partial \boldsymbol{\sigma}} : \mathbb{D}_e : \dot{\boldsymbol{\epsilon}} \leq 0 \tag{6}$$

where $\mathbb{D}_e$ is the fourth order elastic stiffness tensor.

During elasto-plastic loading, the similarity ratio (Hashiguchi [19]) evolves as:

$$\dot{R}_s = U(R_s)\dot{\gamma} \tag{7}$$

$$U(R_s) = \frac{u}{\tan\left(\frac{\pi}{2}R_s\right)} \tag{8}$$

where $U(R_s)$ is a monotonically decreasing function of R_s, and u is a constitutive parameter.

CASM adopts the same hardening rule as the modified Cam-Clay model:

$$\dot{p}'_o = \frac{p'_o}{\lambda^* - \kappa^*}\dot{\epsilon}^p_v \tag{9}$$

where $\lambda^* = \lambda/(1+e_o)$ is the slope of normally-consolidated in a volumetric strain-logarithmic mean stress compression plane.

3 Implicit numerical integration

Two fundamental operations are involved in the integration of the constitutive relations: the state update procedure and the computation of the consistent tangent operator. In order to solve the incremental constitutive problem, in this work, a fully implicit scheme is employed, commonly known as the backward Euler scheme (Neto et al. [20]). The stress integration algorithm consists of two steps namely the elastic predictor and, if the trial state does not satisfy the loading condition defined by subloading plasticity, the plastic corrector.

3.1 Elastic predictor

In the first step, an elastic regime is assumed, where plastic internal variables remain constant. In this work, stress integration is performed in terms of p' and $\mathbf{s}$, as it allows for analytical integration of the volumetric elastic model (see eq. (11)) (Rouainia and Muir-Wood [6]). Assuming an elastic regime, the plastic multiplier is set to zero, i.e. $\Delta\boldsymbol{\gamma}_{n+1} = 0$ and consequently:

$$\epsilon^p_{v_{n+1}} = \epsilon^p_{v_n} \qquad p'_{o_{n+1}} = p'_{o_n} \tag{10}$$

Integrating analytically the volumetric part of the elastic model gives:

$$p'_{n+1} = p'_n \exp\left(\frac{\Delta\epsilon_{v_{n+1}}}{\kappa^*}\right) \tag{11}$$

Whereas deviatoric stresses can be obtained as:

$$\mathbf{s}_{n+1} = \mathbf{s}_n + 2G_{n+1}\Delta\boldsymbol{\epsilon}_{d_{n+1}} \qquad G_{n+1} = \frac{3(1-2\mu)}{2(1+\mu)}\frac{p'_{n+1}}{\kappa^*} \tag{12}$$

where the subscript $n+1$ indicates that all values are obtained at the end of the increment.

Therefore, eq. (10)-eq. (12) defines an explicit approximation of the stress state at $n+1$ obtained using an implicit time marching scheme.

3.2 Plastic predictor

In contrast to the classical elastoplasticity framework, the subloading surface approach replaces, the Kuhn-Tucker conditions with the loading condition (Hashiguchi [19]). Consequently, once the elastic trial predictor has been computed, the loading condition is evaluated to determine the admissibility of the trial state. If the loading condition is not met, a plastic correction becomes necessary. In particular, the plastic correction is only applied in cases where $\partial f/\partial\boldsymbol{\sigma} : \mathbb{D}_e : \dot{\boldsymbol{\epsilon}}$ is positive.

During the plastic corrector step, all equations of the model are discretized using a backward Euler approximation. The discrete form of the flow rule, which separates volumetric and deviatoric plastic strains, can be expressed as:

$$\Delta\epsilon^p_{v_{n+1}} = \Delta\boldsymbol{\gamma}_{n+1}\frac{\partial g}{\partial p'_{n+1}} = \Delta\boldsymbol{\gamma}_{n+1}\left(-m\left(\frac{\sqrt{3}J}{M_\theta p'_{n+1}}\right)^m \frac{1}{p'_{n+1}} + \frac{y(m-1)}{{p'_{n+1}}^2}\right) \tag{13}$$

$$\Delta\boldsymbol{\epsilon}^p_{d_{n+1}} = \Delta\boldsymbol{\gamma}_{n+1}\frac{\partial g}{\partial \mathbf{s}_{n+1}} = \Delta\boldsymbol{\gamma}_{n+1}\left(-m\left(\frac{\sqrt{3}J}{M_\theta p'_{n+1}}\right)^m \frac{1}{J}\right)\frac{\partial J}{\partial \mathbf{s}_{n+1}} \tag{14}$$

where *J* is the second invariant of the deviatoric stress tensor.

Introducing these two equations into the elastic model, we can derive the following approximations for the mean effective stress and deviatoric stress:

$$p'_{n+1} = p'_n \exp\left(\frac{\Delta\epsilon_{v_{n+1}} - \Delta\epsilon^p_{v_{n+1}}}{\kappa^*}\right) \tag{15}$$

$$\mathbf{s}_{n+1} = \mathbf{s}_n + 2G_{n+1}\left(\Delta\boldsymbol{\epsilon}_{d_{n+1}} - \Delta\boldsymbol{\epsilon}^p_{d_{n+1}}\right) \tag{16}$$

The equation describing the evolution of the preconsolidation pressure is integrated analytically. By introducing the definition of the increment of volumetric plastic strains, it can be expressed as:

$$p'_{o_{n+1}} = p'_{o_n} \exp\left(\frac{\Delta\epsilon^p_{v_{n+1}}}{\lambda^* - \kappa^*}\right) \tag{17}$$

Finally, the implicit integration of the differential equation describing the evolution of the similarity ratio, R_s, yields:

$$R_{s_{n+1}} = R_{s_n} + U(R_{s_{n+1}})\Delta\boldsymbol{\gamma}_{n+1} \tag{18}$$

Equation (11) to eq. (18) define a system of non-linear equations, whose residual can be expressed as:

$$\mathbf{r}_{n+1} = \begin{cases} p'_{n+1} - p'_n \exp\left(\frac{\Delta\epsilon_{v_{n+1}} - \Delta\epsilon^p_{v_{n+1}}}{\kappa^*}\right) \\ p'_{o_{n+1}} - p'_{o_n} \exp\left(\frac{\Delta\epsilon^p_{v_{n+1}}}{\lambda^* - \kappa^*}\right) \\ \left(\frac{\sqrt{\frac{3}{2}\mathbf{s}_{n+1}:\mathbf{s}_{n+1}}}{p'_{n+1}M_\theta}\right)^n + \frac{1}{\ln r}\ln\frac{p'_{n+1}}{R_{s_{n+1}}p'_{o_{n+1}}} \\ \mathbf{s}_{n+1} - \mathbf{s}_n - 2G_{n+1}\left(\Delta\boldsymbol{\epsilon}_{d_{n+1}} - \Delta\boldsymbol{\epsilon}^p_{d_{n+1}}\right) \\ R_{s_{n+1}} - R_{s_n} - U(R_{s_{n+1}})\Delta\boldsymbol{\gamma}_{n+1} \end{cases} \tag{19}$$

where the unknown variables are:

$$v_{n+1} = \left[p'_{n+1}, p'_{o_{n+1}}, \mathbf{s}_{n+1}, \Delta\boldsymbol{\gamma}_{n+1}, R_{s_{n+1}}\right] \tag{20}$$

This system of equations is solved iteratively using the Newton-Raphson method, which can be expressed as:

$$v_{n+1} = v_{n+1} + \delta v_{n+1} \quad [\Xi_{n+1}]\,\delta v_{n+1} = -\mathbf{r}_{n+1} \quad [\Xi_{n+1}] = \frac{\partial \mathbf{r}_{n+1}}{\partial v_{n+1}} \tag{21}$$

where $[\Xi_{n+1}]$ represents the partial derivatives of $\mathbf{r}_{n+1}$ with respect to the unknown variables vector v_{n+1}. The iterative process concludes once the norm of the residual falls below a prescribed tolerance, i.e., $\|\mathbf{r}_{n+1}\| < \varepsilon_r$, where ε_r is the tolerance. In this work $\varepsilon_r = 5 \times 10^{-13}$.

The consistent tangent (stiffness) operator is the derivative of the stress with respect to the strain increment, a concept initially proposed by Simo and Taylor [21]. Hence, the incremental stress updating procedure involves linearization, with the purpose of achieving quadratic rates of asymptotic convergence in iterative finite element solutions. This approach is necessary since the continuum stiffness matrix does not guarantee this quadratic convergence (Simo [18]; Simo and Hughes [8]). Equation (22) expresses the consistent tangent operator ($\mathbb{D}_{n+1}$).

$$\mathbb{D}_{n+1} = \frac{\mathrm{d}\boldsymbol{\sigma}_{n+1}}{\mathrm{d}\Delta\boldsymbol{\epsilon}_{n+1}} = \frac{\partial\boldsymbol{\sigma}_{n+1}}{\partial v_{n+1}}\frac{\mathrm{d}v_{n+1}}{\mathrm{d}\Delta\boldsymbol{\epsilon}_{n+1}} = -\frac{\partial\boldsymbol{\sigma}_{n+1}}{\partial v_{n+1}}\left[\frac{\partial\mathbf{r}_{n+1}}{\partial v_{n+1}}\right]^{-1}\frac{\partial\mathbf{r}_{n+1}}{\partial\Delta\boldsymbol{\epsilon}_{n+1}} \tag{22}$$

4 Simulation of laboratory tests

In this section, good-quality laboratory tests conducted on Boston Blue Clay (BBC - Braathen [16]; Pestana et al. [17]) were chosen to demonstrate the performance of the implicit algorithm. To showcase the capabilities of the model, simulations of compression triaxial tests under undrained conditions were conducted in SoilTest (PLAXIS [15]), a module based on a single stress point, i.e., a mesh and the geometric model is not necessary. Additional simulations were conducted using a classical elasto-plastic implementation of CASM (Mánica et al. [13]).

The material parameters used in the simulations are as follows: $\lambda = 0.178$, $\kappa = 0.04$, $\mu = 0.24$, $p'_o = 588.4$ kPa, $r = 3.12$, $n = 1.58$, $m = 2.453$ and $M = 1.353$. The simulations were performed for three different values of initial over-consolidation ratio (OCR): $OCR = 1$, $OCR = 4$ and $OCR = 8$. Moreover, for normally consolidated BBC ($OCR = 1$), the void ratio is $e_o = 0.88$; while for over-consolidated BBC ($OCR = 4$) and ($OCR = 8$) are $e_o = 0.904$ and $e_o = 0.905$, respectively. The parameter controlling the evolution of the similarity ratio is $u = 5$.

Figure 1(a) presents the stress path of the test along with the evolution of deviatoric stress in terms of axial strain. The simulations exhibit good agreement with laboratory tests. It is noted that in the cases over-consolidated

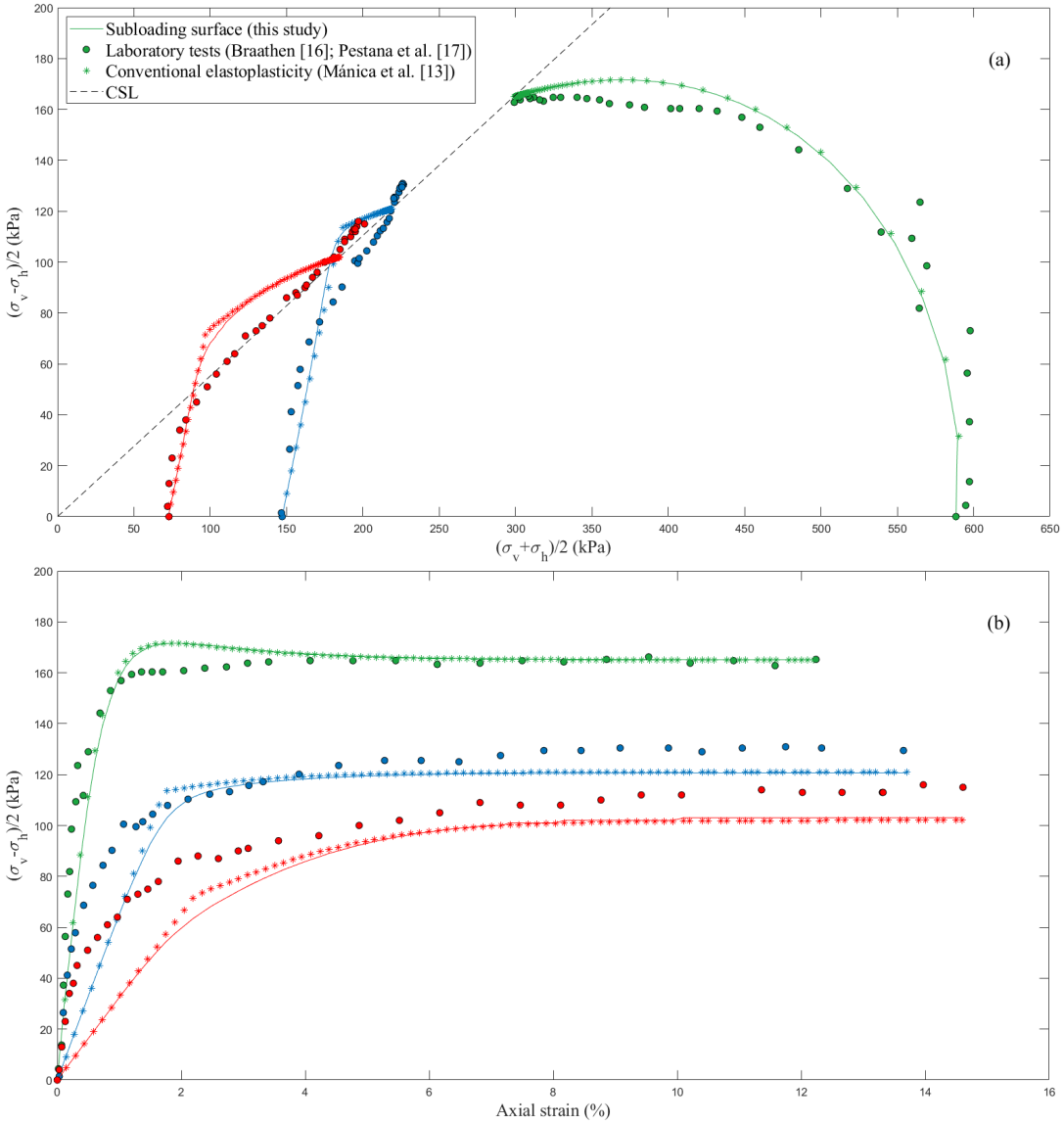

Figure 1. Comparison of predicted and measured undrained triaxial loading behaviour of BBC. $OCR = 1$ (green), $OCR = 4$ (blue) and, $OCR = 8$ (red)

($OCR = 4$) and ($OCR = 8$), the subloading version of CASM accurately predicts a smooth transition from elastic to elasto-plastic regime, a feature observed in the laboratory experiments. It is noted that, σ_v is the vertical stress and σ_h is the horizontal stress.

Finally, in Fig. 1(b), the model prediction is compared to laboratory tests in the deviatoric stress vs. axial strain, ϵ_a, space. The results show that for normally-consolidated BBC, both simulations accurately reproduce the expected behaviour. However, in the case of the over-consolidated BBC, the laboratory tests exhibit deviatoric stress higher than those obtained in the simulations. Nevertheless, the model's implementation ensures a smooth transition in both cases.

5 Conclusions

Implicit integration provides an adequate algorithm for evaluating stress increments within the subloading surface framework. In this study, an implicit stress integration to discretize the constitutive equations of a critical state constitutive model when reformulated using the subloading plasticity approach.

The constitutive model implemented in this work demonstrated the ability to reproduce a smooth transition

from elastic to elastoplastic regime, a characteristic commonly observed in soil behaviour. Numerical simulations of laboratory tests show adequate performance of the model.

Acknowledgements. The study was primarily funded through the 'Beca Generación del Bicentenario' Scholarship Program of the Ministry of Education, Peru. A special thanks to Newcastle University for facilitating the research visit of the first author.

Authorship statement. The authors hereby confirm that they are the sole liable persons responsible for the authorship of this work, and that all material that has been herein included as part of the present paper is either the property (and authorship) of the authors, or has the permission of the owners to be included here.

References

[1] T. Wichtmann, A. Niemunis, and T. Triantafyllidis. Strain accumulation in sand due to cyclic loading: drained triaxial tests. *Soil Dynamics and Earthquake Engineering*, vol. 25, n. 12, pp. 967–979, 2005.
[2] K. Hashiguchi. Constitutive equations of elastoplastic materials with elastic-plastic transition. *Journal of Applied Mechanics*, vol. 47, n. 2, pp. 266–272, 1980.
[3] K. Hashiguchi. Subloading surface model in unconventional plasticity. *International Journal of Solids and Structures*, vol. 25, n. 8, pp. 917–945, 1989.
[4] K. Hashiguchi, K. Saitoh, T. Okayasu, and S. Tsutsumi. Evaluation of typical conventional and unconventional plasticity models for prediction of softening behaviour of soils. *Géotechnique*, vol. 52, n. 8, pp. 561–578, 2002.
[5] K. Hashiguchi. *Foundations of Elastoplasticity: Subloading Surface Model*. Springer Cham, 2017.
[6] M. Rouainia and D. Muir-Wood. Implicit numerical integration for a kinematic hardening soil plasticity model. *International Journal for Numerical and Analytical Methods in Geomechanics*, vol. 25, pp. 1305–1325, 2001.
[7] S. W. Sloan, A. J. Abbo, and D. Sheng. Refined explicit integration of elastoplastic models with automatic error control. *Engineering Computations*, vol. 18, pp. 121–154, 2001.
[8] J. C. Simo and T. J. R. Hughes. *Computational inelasticity*. Springer New York, NY, 1998.
[9] D. M. Pedroso. The subloading isotropic plasticity as variable modulus model. *Computers and Geotechnics*, vol. 61, pp. 230–240, 2014.
[10] P. J. Pinedo, L. Monforte, M. Arroyo, and A. Gens. A subloading surface clay and sand model. In *10th European Conference on Numerical Methods in Geotechnical Engineering (NUMGE2023)*, 2023.
[11] Y. M. A. Hashash and A. J. Whittle. Integration of the modified cam-clay model in non-linear finite element analysis. *Computers and Geotechnics*, vol. 14, n. 2, pp. 59–83, 1992.
[12] H. S. Yu. Casm: A unified state parameter model for clay and sand. *International Journal for Numerical and Analytical Methods in Geomechanics*, vol. 22, n. 8, pp. 621–653, 1998.
[13] M. A. Mánica, M. Arroyo, A. Gens, and L. Monforte. Application of a critical state model to the merriespruit tailings dam failure. *Proceedings of the Institution of Civil Engineers - Geotechnical Engineering*, vol. 175, n. 2, pp. 151–165, 2022.
[14] M. Arroyo and A. Gens. Computational analyses of dam 1 failure at the corrego de feijao mine in brumadinho. Technical report, International Centre for Numerical Methods in Engineering, CIMNE, 2021.
[15] PLAXIS. *PLAXIS 2D Reference Manual*. Bentley Systems International Limited, 2021.
[16] N. F. Braathen. *Investigation of effects of disturbance on undrained shear strength of Boston blue clay*. PhD thesis, Department of Civil Engineering, Massachusetts Institute of Technology, 1966.
[17] J. M. Pestana, A. J. Whittle, and A. Gens. Evaluation of a constitutive model for clays and sands: Part 2 – clay behaviour. *International Journal for Numerical and Analytical Methods in Geomechanics*, vol. 26, pp. 1123–1146, 2002.
[18] J. C. Simo. *Numerical analysis and simulation of plasticity*. Elsevier, vol. 6, 1998.
[19] K. Hashiguchi. Complete formulation of the subloading surface model. In *6th International Conference on Computational Methods for Coupled Problems in Science and Engineering*, 2015.
[20] E. A. S. Neto, D. Perić, and D. R. J. Owen. *Computational Methods for Plasticity: Theory and Applications*. John Wiley and Sons Ltd, 2008.
[21] J. C. Simo and R. L. Taylor. Consistent tangent operator for rate-independent elastoplasticity. *Computer Methods in Applied Mechanics and Engineering*, vol. 48, n. 1, pp. 101–118, 1985.